# Influence of filter layer positions and hydraulic retention time on removal of nitrogen and phosphorus by porous asphalt pavement

Hui Luo, Lin Guan, Zhaoqian Jing, Zeyu Zhang, Xiaobo Hu, Mengni Tao and Yin Wang

## ABSTRACT

This study was aimed to investigate the removal processes of nitrogen (TN), $NH_4^+$-N and phosphorus (TP) from surface runoff by performing experiments on the filter layers in porous asphalt pavement (PAP). Experiments were conducted to compare the differences of the filter layer placed at the top, the middle or the bottom of PAP. The effects of retention time on the removal of the pollutants and the adsorption capacity of PAP materials were also investigated. Results indicated that the filter layer placed under the bed course improved the removal rates of pollutants compared to the other two cases on the whole. The concentration of TP in the effluent decreased by 80% after the 48 h retention time. In conclusion, this study demonstrated that the positions of filter layers and the temporary retention time of surface runoff within the bed course of PAP were critical parameters for determining the removal processes of pollutants. Thus, a certain retention time for surface runoff in bed course is of great importance for PAP to serve as an effective low impact development technology for stormwater management.

**Key words** | filter position, filtration mechanism, porous asphalt pavement, removal of nutrient, surface runoff

**Hui Luo**†
**Zhaoqian Jing** (corresponding author)
**Zeyu Zhang**
**Xiaobo Hu**
**Mengni Tao**
**Yin Wang**
College of Civil Engineering,
Nanjing Forestry University,
Nanjing 210037,
China
E-mail: *zqjing@njfu.edu.cn*

**Lin Guan**†
Nanjing Municipal Design and Research Institute,
Nanjing 210008,
China

†The authors contributed equally to this work.

## INTRODUCTION

In the process of urbanization, regional impervious surfaces were equipped with a large number of roads and rooftops, which in turn led to a significant increase in surface runoff (Ellis *et al.* 2012; Al-Rawas *et al.* 2015). Surface runoff typically contained various pollutants that could reduce the qualities of urban water resources, including total suspended solids (TSS), nutrients such as phosphorus (TP) and nitrogen (TN), hydrocarbons, and heavy metals (Kayhanian *et al.* 2012). Among multiple available techniques for managing surface runoff, especially those applied in an urban environment, porous asphalt pavement (PAP) was considered as the most promising solution to the dual problems of increased urban surface runoff and decreased quality (Bentarzi *et al.* 2016). PAP, which was mainly comprised of porous asphalt, could serve as a subcrust for porous asphalt concrete (PAC) above a base course, where an open-graded aggregate bed with various depths depending on water storage requirements (Huang *et al.* 2016) and frost depths (Ferguson 2005) could be involved. Permeable geotextile membranes, which were generally paved within PAP with one or two layers for road strengthening, could also separate each layer and prevent the migration of stones and gravel (Mullaney *et al.* 2012; Scholz 2013; Nnadi *et al.* 2014). Throughout the infiltration process, surface runoff would be processed by various steps, including mechanical filtration, physical sorption, chemical sorption (Zhao & Zhao 2014), desorption, nutrient transformation, degradation (Drake *et al.* 2013), and chemical precipitation (Myers *et al.* 2011).

There were several methods for improving the purification efficiency of surface runoff by PAP, such as altering mix ratios, void ratios or infiltration rates of surface asphalt mixture (Huang *et al.* 2016), changing subbase materials and mix ratios of base layers (Xie *et al.* 2019), adding aquifer (Zhao & Zhao 2014) or using a geotextile layer (Zhao *et al.* 2018), reasonably utilizing subcrust materials (Liu *et al.* 2018), etc. Among these methods, application of inverted filter layers was defined as the most efficient and economical method. Multiple studies have confirmed that

doi: 10.2166/wst.2020.110

a standard PAP paved with a geotextile layer could significantly improve the quality of stormwater runoff that seeps into the soil (Dietz *et al.* 2017). Moreover, application of filter layers in pavements, gravels or bedding courses could contribute to the quality improvement of rainwater by absorbing organic pollutants, heavy metals (Nnadi *et al.* 2014), and chlorides (Jiang *et al.* 2015), and retaining rainwater simultaneously. Notably, PAP which included a geotextile membrane in the bottom of the cushion layer could cause a decrease in TN content by no more than 30%. TN species mainly existed as nitrate in infiltrate. In contrary to the TN results, ortho TP concentrations were significantly lower in the PAP infiltrate (Brown & Borst 2015). Nevertheless, up to 47% of TN could be removed when filter layers were paved in the middle of a PICP system (Drake *et al.* 2013). Several laboratory-based experiments showed that the presence of geotextile layers significantly influenced the removal efficiency of ammonia-nitrogen and ortho-TP-phosphorus by 84.6% and 77.5%, respectively (Maharaj & Elefsiniotis 2001). A test on 16 pollutant indices in influent and effluent samples showed that geotextiles when paved on the top of soil exerted limited effects on removing TP, $Cl^-$ and TN but remarkable effects on removing Cu, Zn, Pb and Cd (Jiang *et al.* 2015). A laboratory-scale PAP system in which geotextiles were paved at the bottom had been well established. Then, the research results based on the system demonstrated that the average removal rates of SS reached 79.8–98.6% for all layers with the 'sieving action' mainly occurring in geotextiles, while the average removal rates of TP were 54.8–72.1%. $NH_4^+$-N and TN could not be stably removed by layers and geotextiles (Niu *et al.* 2016; Selbig *et al.* 2019). A pilot test program in a field study of the PICP system had been conducted with and without a geotextile in the top of soil-base and the results indicated that the presence of a top geotextile improved the removal of TP and Pb from surface runoff (Mullaney *et al.* 2012; Jayakaran *et al.* 2019).

Previous studies mainly focused on the effects of materials and types of PAP on the filtration of surface runoff, whereas few studies referred to the direct impacts of the positions of geotextiles on the quality of surface runoff. Only a recent research preliminarily compared the measured values of PAP with and without a geotextile layer (Zhao *et al.* 2018). In general, the impacts of geotextiles with different positions on the removal of nutrients from surface runoff were not comprehensively discussed in previous studies (Kuruppu *et al.* 2019). Thus, in this study, a laboratory test was performed by collecting abundant data and providing convincing evidence to reveal the role of geotextile membranes within PAP and to optimize their applications in road designs and acquire a better quality of surface runoff.

In this study, the influences of filter layer positions on the removal of TN, TP, $NH_4^+$-N were investigated based on PAP systems. The aims of this study were to evaluate the effects of a filter layer within a PAP and to investigate the differences of PAPs that embedded with non-woven fabrics at the top, middle or bottom in removing TN, TP, $NH_4^+$-N from surface runoff. Moreover, the mechanisms underlying the removal of surface runoff by PAPs were explored.

## MATERIALS AND METHODS

The experiment was conducted in two stages: the first stage was to monitor the removal efficiency of pollutants by PAP during artificial rainfall event 1; the second stage involved a temporary storage period (48 h) of the stormwater that was generated by artificial rainfall event 2 and stored within the reservoir course to analyze changes in removal efficiency.

### Materials

#### PAP models

The PAC specimen used in this study was a mixture of bitumen with high adhesion, crushed basalt aggregates and limestone powder. The mixture was prepared by Marshall compaction (50 blows per side) according to the Technical Specifications for Permeable Asphalt Pavement (CJJ/T 190-2012) in China, the void content of the specimen was kept at around 20.4%. The gradation of the specimen was shown in Table 1. Crushed basalt aggregates and natural sand were used as the graded gravel and cushion layer; the gradation was shown in Tables 2 and 3. The fineness

**Table 1** | The gradation of the PAC specimen for testing

| | Passing rate (by mass) under different sieve sizes (mm)/% | | | | | | | | | | |
|---|---|---|---|---|---|---|---|---|---|---|---|
| **Mixture** | **16** | **13.2** | **9.5** | **4.75** | **2.36** | **1.18** | **0.6** | **0.3** | **0.15** | **0.075** | **Binder content (%)** |
| PAC-13 | 100 | 94.5 | 66.1 | 23.6 | 16.9 | 12.8 | 10.7 | 8.1 | 6.6 | 4.9 | 4.8 |

PAC-13 is a common aggregate gradation for surface courses that are designed with a maximum particle size of 16 mm.

**Table 2** | The gradation of the graded gravel for testing

| Size of mesh (mm) | 26.5 | 19 | 16 | 13.2 | 9.5 | 4.75 | 2.36 | 1.18 | 0.6 | 0.3 | 0.15 |
|---|---|---|---|---|---|---|---|---|---|---|---|
| Graded gravel (%) | 94.4 | 76.2 | 65.3 | 56.4 | 48.8 | 34.3 | 24.4 | 17.3 | 10.1 | 4.3 | 2.9 |

**Table 3** | The gradation of the natural sand for testing

| Sieve size (mm) | 9.5 | 4.75 | 2.36 | 1.18 | 0.6 | 0.3 | 0.15 |
|---|---|---|---|---|---|---|---|
| Passing rate (%) | 100 | 93.8 | 85.6 | 79.3 | 65.4 | 19.2 | 2.1 |

modulus of the natural sand was 2.41 and the bulk specific gravity was 2.64 g/cm$^3$. The void content of air was 38.8% under stacking state, which was in accordance with Chinese specification JTG E42-2005. Geotextiles were used as filter layer in the tests, the main properties of the non-woven geotextiles were listed in Table 4. Three PAP models were constructed in this study. The non-woven permeable geotextile membranes were placed at the top in order to separate the PAP from the graded gravel course, or placed in the middle or bottom of the bed course (Figure 1).

## Synthetic rainwater

The pollutant purification by PAPs could be influenced by multiple factors, such as compositions and pollutant loads of surface runoff, site-specific conditions, weather conditions, PAP designs, maintenance services, etc. (Maniquiz-Redillas & Kim 2016). The types and concentrations of different pollutants in runoff rainwater were selected based on an investigation of rainwater runoff in Nanjing, Jiangsu, China (Table 5). The chemicals for surface runoff and influent components were shown in Table 6.

**Table 4** | The properties of geotextiles

| Property | Test result | Test method |
|---|---|---|
| Mass per unit area (g/m$^2$) | 194.7 | ISO 9864 |
| Thickness/under pressure of 2 kPa (mm) | 1.317 | ISO 9863 |
| Tensile strength (kN/m) | 11.2 | ISO 10319 |
| Rate of elongation (%) | 43.1 | ISO 10319 |
| CBR bursting strength (N) | 1,723 | ISO 12236 |
| Permeability (mm/s) | 1.18 | ISO 11508 |

## Rainfall design

In the study, an artificial rainfall event with a total precipitation of 59.71 mm, 0.63 mm/min, a rainfall duration of 120 min and a return period of 5 years were designed according to the rainstorm intensity formula of Nanjing (Equation (1)). The well-known Chicago method (Silveira 2016) was used to design the distribution of the simulated rainfall event. As shown in Figure 2, the rainfall event was characterized by a total duration of 120 min, a time step of 5 min, a return period of 5 years, and $\gamma$ of 0.40.

$$i = \frac{64.3 + 53.8 \times \log P}{(t + 32.9)^{1.001}} \quad (1)$$

Before peak:

$$i(t_b) = \frac{A\left[\frac{(1-n)t_b}{r}\right] + b}{\left[\frac{t_b}{r} + b\right]^{n+1}} \quad (2)$$

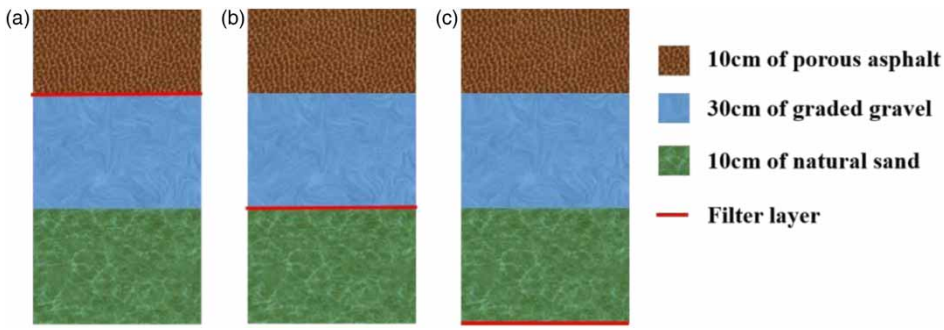


**Figure 1** | A simplified schematic cross section of PAPs with a geotextile layer at the top (a), middle (b) or bottom (c).

**Table 5** | The EMC of pollutants from different rainfall events (mg/L)

| Sampling date | Dry period prior to sampling date (h) | $EMC_{TP}$ | $EMC_{TN}$ | $EMC_{NH_4\text{-}N}$ |
|---|---|---|---|---|
| 2017.3.19 | 147 | 1.14 | 11.48 | 7.28 |
| 2018.5.25 | 71 | 1.09 | 9.87 | 6.37 |
| 2018.8.12 | 196 | 1.28 | 12.74 | 8.41 |
| 2018.11.5 | 98 | 0.82 | 10.36 | 5.26 |

**Table 6** | Synthetic rainwater distribution water quality

| Type of pollutants | Concentration of synthetic rainwater (mg/L) | Chemical reagent |
|---|---|---|
| TP | 2.6 | $KH_2PO_4$ |
| TN | 15.82 | $KNO_3$, $NH_4Cl$ |
| $NH_4^+$-N | 10.65 | $NH_4Cl$ |
| $NO_3$-N | 5.17 | $KNO_3$ |

After peak:

$$i(t_a) = \frac{A\left[\frac{(1-n)t_a}{1-r} + b\right]}{\left[\frac{t_a}{1-r} + b\right]^{n+1}} \quad (3)$$

where i (mm/min) is the rainfall intensity, t (min) is the rainfall duration, P is the recurrence interval, and A, b, and n are the constants dependent on the units employed and the recurrence interval of the storm.

## Artificial rainfall system

An artificial rainfall system, which was comprised of a tank, a pump, a nozzle system, an electronic flow meter, and a flow controller, was designed for setting the stage for the application of synthetic rainwater in all tests (Figure 3). A primary pipe with a diameter of 2.5 cm was used to connect the pump in the tank to the nozzle system. The nozzle system was connected by flexible tubing. The flow rates of simulated rainfalls were measured and controlled by a flow meter and a flow controller.

## Methods

### Adsorption experiments

The batch sorption experiment was performed to draw the adsorption isotherms of TP and TN in the raw materials. 5 g adsorbent was mixed with 100-mL TP and TN of different concentrations in 250-mL conical flasks. The concentrations of TP and TN ranged from 10 to 100 mg/L and 5 to 90 mg/L (pH 7.0), respectively. Then, all the conical flasks were shaken at 150 rpm and 25 °C for 24 h.

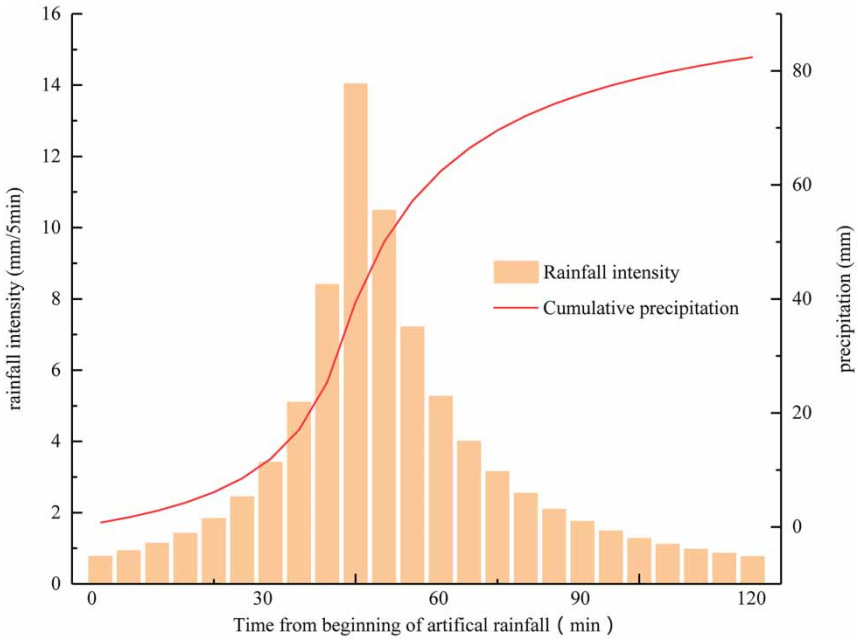


**Figure 2** | Typical rainfall process.

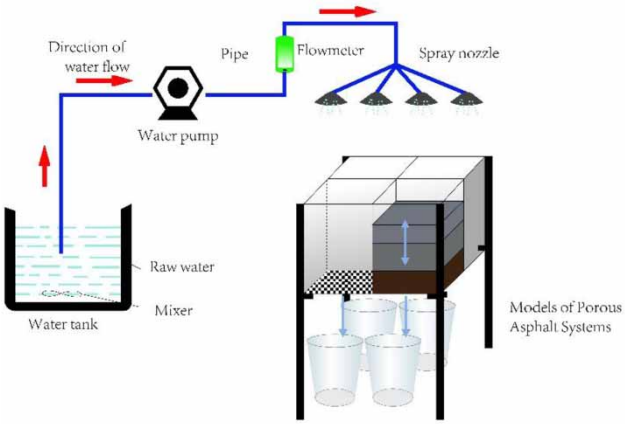


**Figure 3** | A schematic diagram of the experimental setup.

### Artificial rainfall tests

Rainfall stimulations were performed twice based on the laboratorial rainfall system. All three PAP models were tested during the first artificial rainfall, and only the model with the best performance in pollutant removal was tested again in the second rainfall event. The bottom hole was open during the first rainfall test but closed during the second rainfall test except for sampling. Time counting started immediately when the artificial rainfalls began. Subsequent effluent samples were then collected at predetermined sampling times.

### Statistical analysis

The TN removal efficiency was calculated according to Equation (2),

$$R = (1 - C_{out}/C_{in}) \times 100\% \quad (4)$$

where R was the pollutant removal efficiency (%), $C_{in}$ and $C_{out}$ were the average pollution concentration of the inflow (mg/L) and outflow (mg/L), respectively.

## RESULTS

### Effects of filter layer position on initial outflow

The efficiencies of pollutant removal from surface runoff by three test rigs during the artificial rainfall events were shown in Table 7. Compared to the test rig A, there was a 4-min delay in the effluent time of the test rig C. The effluent in the test rig C occurred three minutes after the surface runoff discharge from the test rig B with a geotextile membrane paved at the middle layer. The results showed an obvious decrease in the contents of $NH_4^+$-N, TN and TP in the initial effluent. The mean concentration of $NH_4^+$-N, TN and TP in the initial infiltrate sample was 3.41 mg/L, 13.52 mg/L and 1.5 mg/L, which was 67.93%, 15.82% and 57.25% lower than that in the synthetic rainwater, respectively. Intriguingly, the removal efficiencies of pollutants varied significantly among three groups. In the test rig C, a non-woven geotextile membrane was paved at the bottom layer, which caused a highest removal efficiency of $NH_4^+$-N. The removal efficiencies of TN were similar among three groups, while the test rig B that performed the worst in TN removal. In terms of TP, the removal efficiencies ranged from 25.4% to 52.1% and reached the highest in the test rig A where a geotextile was placed at the top layer. But, the analysis of variance indicates that the position of a geotextile layer in the PAP system didn't result in a statistically significant difference with respect to the removal of $NH_4^+$-N, TN and TP from the initial influent ($p$ value equal to 0.1).

### The removal process during an artificial rainfall event

During the first artificial rainfall event, the removal rates of $NH_4^+$-N, TN and TP were shown in Figure 4. There was an obvious difference in the removal rates between three test rigs with geotextile layers in different positions. Results showed that the test rig C showed the highest efficiency in removing TN from the infiltrate samples, while the test rig A showed the best efficiency in removing TP. The average

**Table 7** | Information about the initial effluent

| | | | Concentration (mg/L) | | | Removal rate (%) | | |
|---|---|---|---|---|---|---|---|---|
| Test rig | Geotextile position | Effluent time (min) | $NH_4^+$ | TN | TP | $NH_4^+$ | TN | TP |
| A | Top | 17 | 3.69 | 14.18 | 1.52 | 65.35 | 10.37 | 51.98 |
| B | Middle | 18 | 3.43 | 14.52 | 1.67 | 67.77 | 8.22 | 36.26 |
| C | Bottom | 21 | 3.12 | 11.87 | 1.31 | 70.67 | 24.97 | 41.91 |

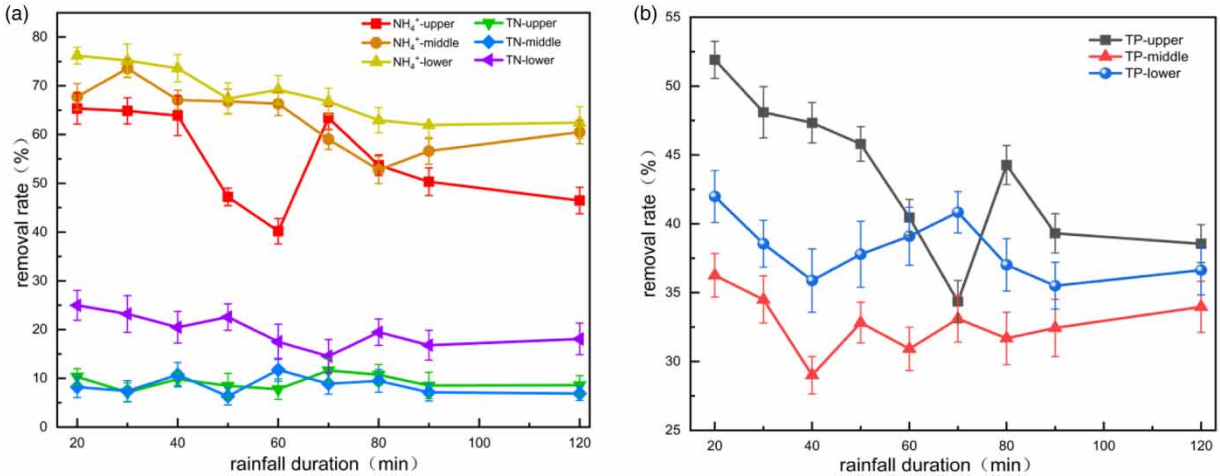


**Figure 4** | Results of the first artificial rainfall event. (a) The removal rates of $NH_4^+$ and TN by the PAP, where A1, B1 and C1 represented the removal rates of $NH_4^+$ and A2, B2 and C2 represented the removal rates of TN. (b) The removal rates of TP by the PAP.

removal rate of TP by the test rig A was about 13.1% higher than that by the test rig B at the end of event and about 5.3% higher than that by the test rig C. After a 120-min artificial rainfall, the test rig C with a filter layer in the bottom of the PAP exhibited the best removal effect on TN, while the test rig A that contained a geotextile layer in the top of the PAP was defined as the most efficient remover for TP. All these results suggested that the positions of geotextiles could significantly influence the removal effects on pollutants from surface runoff.

## The removal efficiencies of the PAP with retention function

The results in Figure 5 showed that the concentrations of $NH_4^+$-N, TN and TP with a non-woven geotextile in the bottom of the PAP during the second rainfall. On the contrary to the results from the 120-min artificial rainfall event, there was an obvious change in the removal rate of pollutants during the 48-h residence. The concentration of TP in the runoff decreased obviously in the initial 8 h, then continuously decreased with the residence time, and remained relatively stable in the last 24 h. Notably, more than 82% of TP was removed from the surface runoff by PAP when the storage time reached 48 h. The remove rate of $NH_4^+$-N increased at the first 16 h but decreased in the later 36 h to the final removal rate of about 75%. The concentration of TN remained relatively stable and only about 25% were removed. The results concluded that the PAP that could retain runoff for a certain time performed more effectively in removing TP by nearly 20% than the PAP that could not retain runoff.

## The adsorption capacities of the materials used in PAP

The adsorption isotherms that demonstrated the adsorption quantity of TN and TP in asphalt mixture, graded gravel and natural sand were shown in Figure 6. It was observed that under the ammonium-free condition, the adsorption capacities of asphalt mixture, graded gravel and natural sand to TP increased with the equilibrium concentrations of TP. Figure 6 also showed that the adsorption capacities to TP of three type of materials enhanced in the following order: graded gravel, natural sand and asphalt mixture. These results indicated that in the absence of ammonium, asphalt mixture in the top layer of PAP showed the strongest adsorption capacity to TP, while graded gravel and natural sand showed weak adsorption capacities to TP.

The data about equilibrium adsorption were further analyzed by the Freundlich and Langmuir isotherm models. The adsorption isotherm parameters of TP by graded gravel, natural sand and asphalt mixture including correlation coefficient ($R^2$) were calculated and shown in Table 8. According to the results, all the values of $R^2$ were larger than 0.83, implying that the Freundlich and Langmuir isotherm models fully interpreted the equilibrium adsorption data. The $K_f$ values for TP decreased by the following order: asphalt mixture, natural sand and grade gravel, while the $K_f$ values for TN decreased by the order of natural sand, grade gravel and asphalt mixture. These results indicated that asphalt mixture exhibited the strongest adsorption capacity to TP, while grade gravel showed the weakest adsorption capacity. Notably, natural sand with the highest $K_f$ value showed the strongest removal capacity

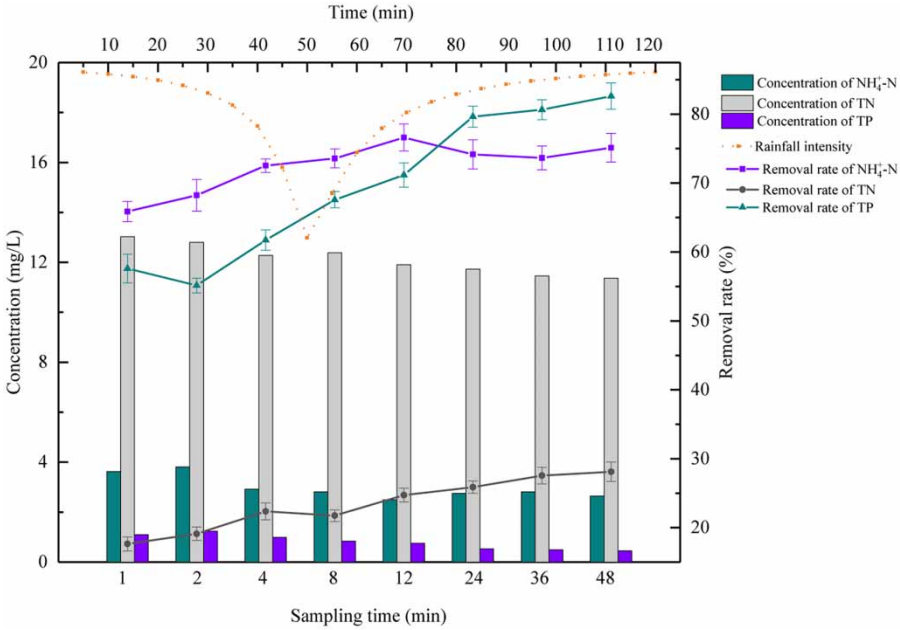


**Figure 5** | The concentrations and removal rates of second artificial rainfall event on the PAP providing 48 h stormwater storage.

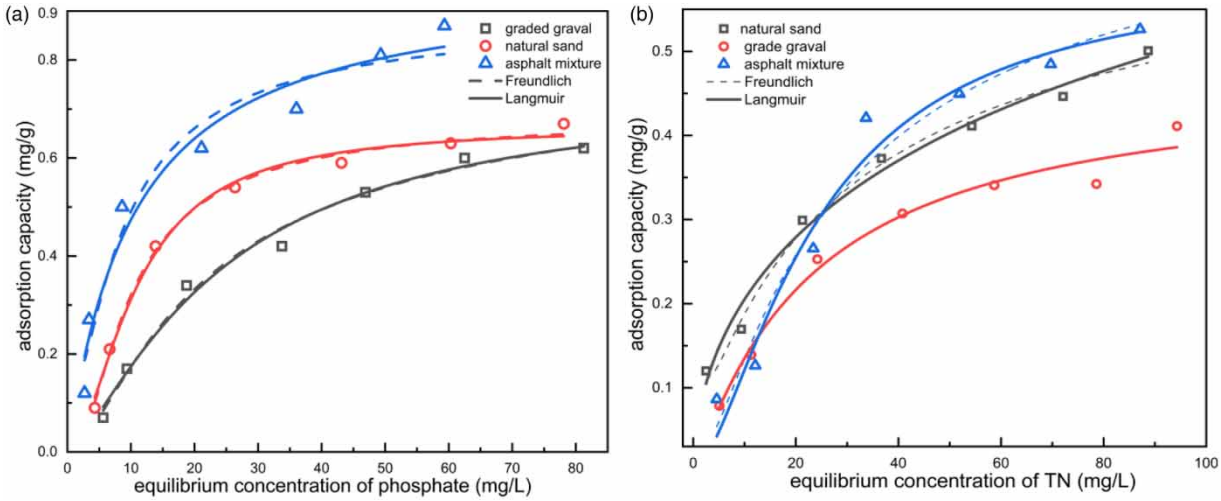


**Figure 6** | The adsorption isotherms of TP (a) and TN (b) in graded gravel, natural sand and asphalt mixture (the initial concentration of TP: 10–100 mg/L, TN of 5–90 mg/L; pH: 7.0; contact time: 24 h).

to TN, while asphalt mixture with the lowest $K_f$ value showed the weakest sorption capacity.

## DISCUSSION

### Differences in initial effects of filter layers between PAP

The geotextile membranes in PAP could have direct effects on hydraulic function because of the lower permeability of geotextile layers when compared to other pavement layers. Further, based on the finding that there was a 5-min delay in the initial effluent between a geotextile membrane in the top layer of PAP and a geotextile membrane in the bottom layer of the PAP, postulated that the geotextile membranes with different positions in PAP could exhibit distinct hydraulic effects. The removal rates of $NH_4^+$-N and TN by the test rig C were highest, while the test rig A showed the most significant effect on TP removal from the initial outflow. It was speculated that the different positions of geotextiles and the

**Table 8** | The isotherm parameters of TP adsorption by graded gravel, natural sand and asphalt mixture

| Isotherm model | | Parameters | Graded gravel | Natural sand | Asphalt mixture |
|---|---|---|---|---|---|
| TP | Freundlich | $k_f/(L\cdot g^{-1})$ | 0.025 | 0.057 | 0.11 |
| | | 1/n | 0.77 | 0.62 | 0.55 |
| | | $R^2$ | 0.91 | 0.83 | 0.85 |
| | Langmuir | $Q_m/(mg\cdot g^{-1})$ | 0.43 | 0.82 | 1.16 |
| | | $b/(L\cdot mg^{-1})$ | 0.079 | 0.059 | 0.058 |
| | | $R^2$ | 0.97 | 0.98 | 0.93 |
| TN | Freundlich | $k_f/(L\cdot g^{-1})$ | 0.037 | 0.078 | 0.030 |
| | | 1/n | 0.55 | 0.42 | 0.67 |
| | | $R^2$ | 0.95 | 0.97 | 0.93 |
| | Langmuir | $Q_m/(mg\cdot g^{-1})$ | 0.03 | 0.019 | 0.017 |
| | | $b/(L\cdot mg^{-1})$ | 17.6 | 24.5 | 48.7 |
| | | $R^2$ | 0.97 | 0.96 | 0.94 |

relatively short retention duration were main reasons contributing to these results (Niu *et al.* 2016). In the test rig A, surface runoff was mainly stored in the asphalt layer. As shown in Figure 6 and Table 8, both the adsorption saturation and adsorption rate of TP by asphalt mixture were higher than the other elements. In addition, the removal rate of TP reached the highest in the initial effluent.

The adsorption capacity of asphalt mixture to TN and $NH_4^+$-N was worse than that of nature sand (Huang *et al.* 2016). Thus, surface runoff would rapidly penetrate the asphalt mixture layer and accumulate in the gravel layer when a geotextile membrane was paved in the middle layer of PAP, which explained why the concentrations of TN and $NH_4^+$-N in the initial effluent were higher in the test rig B than in the test rig A and C. The results suggested that the PAP with a filter layer at the bottom structure could separate the cushion from the sub-grade more effectively and achieve a higher removal efficiency of pollutants from the initial runoff. Several processes that occurred within PAP could be reasons for the reductions in the concentrations of TN, TP, $NH_4^+$-N in the effluent samples, including the adsorption of materials in the air voids within pavement layers (such as the bitumen in the porous asphalt mixture and the natural sand in the bedding course) (Jiang *et al.* 2015), the precipitation between ion exchange and mineral within the bedding course, and the retention of pollutants by filter layers (Zhao *et al.* 2018).

## The direct drainage of surface runoff by PAP

### The influence of filter layer positions on nitrogen removal

During the 120-min artificial rainfall, the test rig C showed the highest removal rate of TN and $NH_4^+$-N, while the test rig A performed the best in removing TP, which was consistent with the research by Drake *et al.* that investigated the water qualities of a PAP system in Ontario from spring to fall (Drake *et al.* 2013). These results could be mainly caused by the different positions of filter layers and the relatively short duration of residence time. The infiltration rate of surface runoff in the filter layer was much lower than that in the natural sand that had a 38.8% void space. Thus, the flow rate of surface runoff would be sharply reduced on the surface of the filter layer when surface runoff flowed through the natural sand and entered the filter layer. This character also extended the residence time of surface runoff in the natural sand before the discharge of surface runoff and facilitated the interaction between TN, $NH_4^+$-N and the natural sand in the bedding course.

According to several previous studies (Welker *et al.* 2012; Sdiri & Bouaziz 2014), the adsorption of TN occurred with the dissolution of sand surfaces at the mineral-surface runoff interface within the bedding course of PAP which contained a geotextile layer at the bottom. This led to the formation of adsorption on the surface and sand holes and the decrease in TN concentration in the outflow (Eck *et al.* 2012). However, the filter layer paved between the base course and the surface layer could not improve the removal capacity of TN because this type of PAP could not alter the retention time for surface runoff and the natural sand within the bedding course. TN was mainly removed by a certain amount of microorganisms through ammoniation in the aerobic environment (Jiang *et al.* 2015). An aerobic environment could be created within the upper subsurface aggregate layers of these systems by draining the permeable pavements. This environment would trigger the nitrification of $NH_4^+$-N to $NO_3^-$-N and lead to a decrease in $NH_4^+$-N concentration. Nevertheless, the concentration of TN still remained high for that the removal of nitrogen in surface runoff was not mainly based on adsorption (Henderson & Tighe 2011). Altogether, the removal efficiency of TN remained low during the infiltrate process occurring within PAP.

### The influence of filter layer positions on TP removal

The TP concentrations decreased after water samples had infiltrated through PAP. Besides, all the tests showed a downward tendency with the sampling time. In general, the PAP that contained a filter layer at the top was more efficient in TP removal when compared to the test rigs A and B, which could attributed to the relatively short residence duration of surface runoff in asphalt mixture. A prior study on the topography of asphalt indicated that the surface of

asphalt showed typical alveolate structure (Zhang 2014), which was caused by the interaction among asphaltenes, colloids and paraffins. The scale of alveolate structure could partly reflect the roughness of asphalt surface. The adsorption sites on asphalt surface were 'open' when rainwater hit the pavements. Thus, several polar components in asphalt, such as carboxyl and hydroxyl groups in oxygenated chemicals like carboxylic acids and phenols, could provide plentiful mobile free electrons and generated a strong adsorption capacity to phosphate anion ($PO_4^-$). In addition, the air void of surface course is less than that of choker course, which led to a slower infiltration rate of rainwater in surface course and a longer exposure time to rainwater. Hence, the absorption capacity of choker course was lower than that of surface course when the filter layer was paved in the middle of PAP. TP was normally removed by the materials of PAP via adsorption, filtration, and precipitin reaction (Drake *et al.* 2013).

## PAP retains surface runoff for a retention time

The removal efficiency of the test rig C when surface runoff was directly discharged was lower than that when surface runoff could be temporarily retained. In addition, there was a strong power function correlation between the removal rates of TP and the retention time, indicating that the residence time directly influenced the removal process of TP.

These apparent changes could possibly be caused by the sorption processes of TP occurring within the materials of PAP. A previous study confirmed that the removal of phosphorus from surface runoff was based on both adsorption and ion exchange that was closely related to the dissolution of the material surface (Eck *et al.* 2012). The surface adsorption of all materials in surface runoff under an acidic condition (initial pH = 3.7) constituted the first step for the removal of pollutants and led to a rapid increase in the pH and the conductivity of surface runoff. Moreover, the removal rates increased with the pH levels. The enhances in the removal of pollutants when pH > 5.1 were attributed to the precipitation of carbonate that led to a higher removal capacity of PAPs (Drake *et al.* 2013). Thus, the removal process was predominantly governed by the precipitation of adsorption and ion exchange since the pH of surface runoff remained above 5.1 for more than 32 hours during the 48-h retention.

Scanning electron microscopy (SEM) with the energy dispersive spectrum (EDS) analysis were performed in the tests, compared to Figure 7(a), the surface of basalt aggregates before the experiments was smoother. However, after the 48 h of residence time in temporary storage, a remarkable change in the surface structure was observed, where polyhedral crystal aggregates and phosphate precipitates were formed due to the phosphorus adsorption on the surface (Figure 7(b)). Similar findings of the formation of precipitates on the surface of the materials were observed in the previous studies (Okochi 2013). According to the EDS results, the major elements on the surface of basalt aggregates were found to include calcium, iron, aluminum and silicon (Figure 8(a)). It was noted that, after the storage time, the EDS peak intensities of several elements such as aluminum and iron in basalt aggregates were diminished (Figure 8(b)). The formation of phosphorus peak in basalt aggregates after the storage experiments indicated that phosphate precipitates were formed on the surface of basalt aggregates.

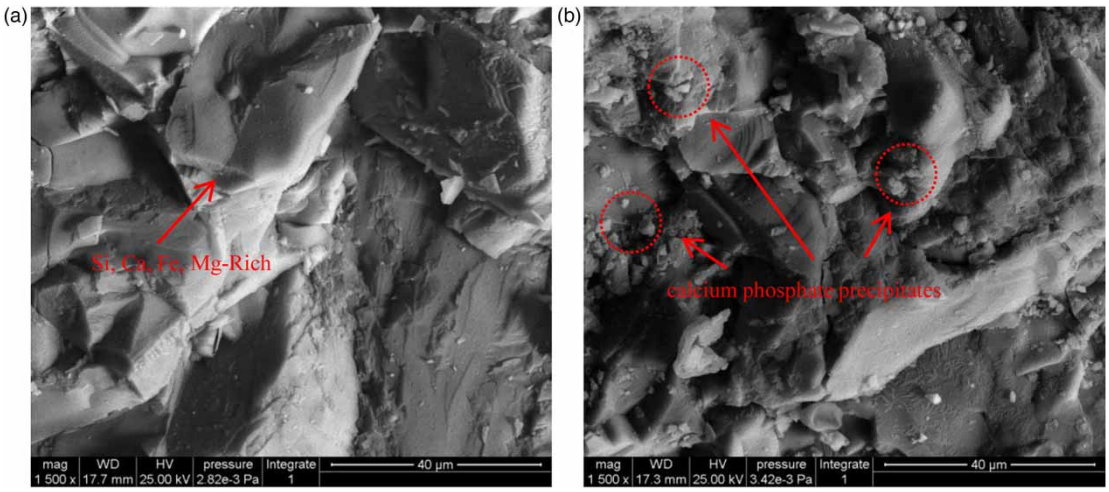


**Figure 7** | SEM images of basalt aggregates before the experiments (a) and after the tests (b).

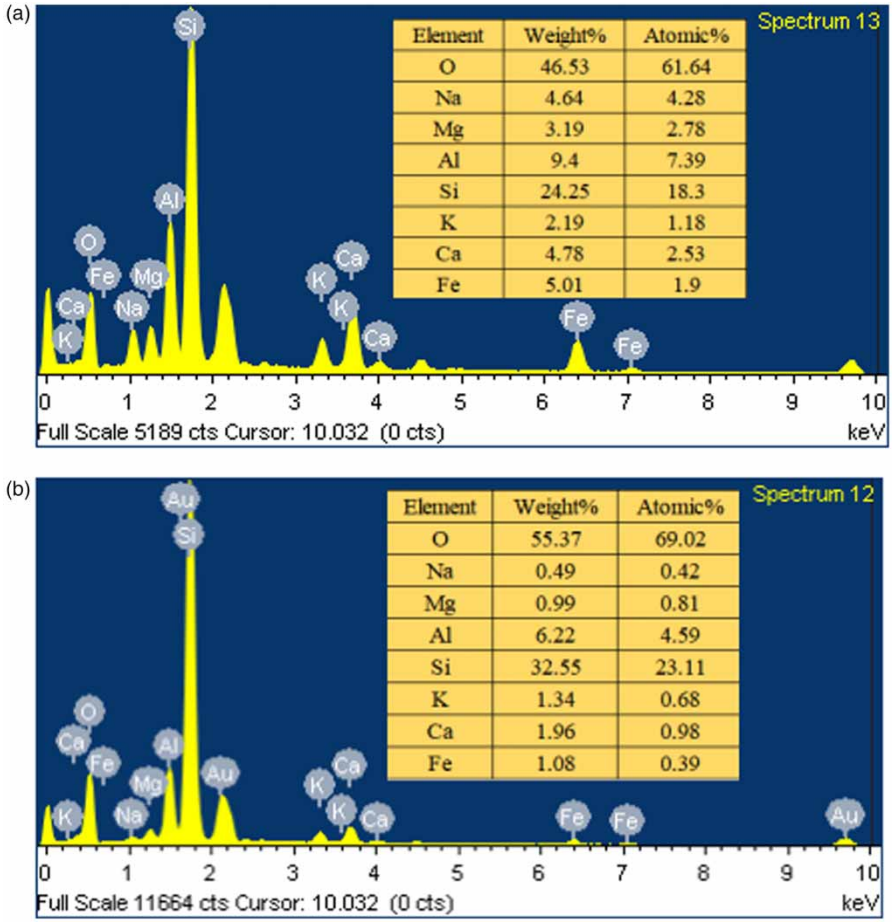


**Figure 8** | EDS results of basalt aggregates as received (a) and after experiments (b).

## CONCLUSIONS

In the current work, laboratory experiments were performed for investigating the removal efficiencies of pollutants from surface runoff based on PAP systems with filter layers at different positions. An additional design parameter was included in the experiments for dealing with surface runoff detention when direct drainage of stormwater was constrained to provide a retention. The decreased concentrations of pollutants in the initial effluent suggested that the removal efficiencies of TN, TP and $NH_4^+$-N from the initial surface runoff were less affected by the application of filter layers in PAP systems. Our results indicated that the presence of filter layers within PAP systems could not alter the tendencies for TN, TP and $NH_4^+$-N over time but could improve the removal rates. Herein, placing a non-woven geotextile membrane at the bottom of a PAP system could be recommended as an appropriate approach to increasing the removal efficiencies of TN, TP and $NH_4^+$-N. In addition, the PAP which provide a 48-h retention time showed a higher removal capacity of pollutants. These results indicated that a certain retention time for surface runoff could enhance the performance of a PAP system in managing stormwater as a low impact development technology.

## ACKNOWLEDGEMENTS

This study was supported by the National Science and Technology Support Program (2015BAL02B04), the Technology Project of China Housing and Urban Rural Development Ministry (2015-K7-012) and a project funded by the Priority Academic Program Development of Jiangsu Higher Education Institutions (PAPD).

## REFERENCES

Al-Rawas, G. A., Valeo, C., Khan, U. T. & Al-Hafeedh, O. H. 2015 Effects of urban form on wadi flow frequency analysis in the

Wadi Aday watershed in Muscat, Oman. *Urban Water Journal* **12** (4), 263–274.

Bentarzi, Y., Ghenaim, A., Terfous, A., Wanko, A., Feugeas, F., Poulet, J. B. & Mosé, R. 2016 Hydrodynamic behaviour of a new permeable pavement material under high rainfall conditions. *Urban Water Journal* **13** (7), 687–696.

Brown, R. A. & Borst, M. 2015 Nutrient infiltrate concentrations from three permeable pavement types. *Journal of Environmental Management* **164**, 74–85.

Dietz, M. E., Angel, D. R., Robbins, G. A. & McNaboe, L. A. 2017 Permeable asphalt: a new tool to reduce road salt contamination of groundwater in urban areas. *Ground Water* **55** (2), 237–243.

Drake, J. A. P., Bradford, A. & Marsalek, J. 2013 Review of environmental performance of permeable pavement systems: state of the knowledge. *Water Quality Research Journal of Canada* **48** (3), 203–222.

Eck, B. J., Winston, R. J., Hunt, W. F. & Barrett, M. E. 2012 Water quality of drainage from permeable friction course. *Journal of Environmental Engineering-ASCE* **138** (2), 174–181.

Ellis, J. B., Revitt, D. M. & Lundy, L. 2012 An impact assessment methodology for urban surface runoff quality following best practice treatment. *Science of the Total Environment* **416**, 172–179.

Ferguson, B. K. 2005 *Porous Pavements*. CRC Press, Boca Raton, FL, USA.

Henderson, V. & Tighe, S. L. 2011 Evaluation of pervious concrete pavement permeability renewal maintenance methods at field sites in Canada. *Canadian Journal of Civil Engineering* **38** (12), 1404–1413.

Huang, J., Valeo, C., He, J. X. & Chu, A. 2016 Three types of permeable pavements in cold climates: hydraulic and environmental performance. *Journal of Environmental Engineering* **142** (6), 04016025.

Jayakaran, A. D., Knappenberger, T., Stark, J. D. & Hinman, C. 2019 Remediation of stormwater pollutants by porous asphalt pavement. *Water* **11** (3), 520.

Jiang, W., Sha, A. M., Xiao, J. J., Li, Y. L. & Huang, Y. 2015 Experimental study on filtration effect and mechanism of pavement runoff in permeable asphalt pavement. *Construction and Building Materials* **100**, 102–110.

Kayhanian, M., McKenzie, E. R., Leatherbarrow, J. E. & Young, T. M. 2012 Characteristics of road sediment fractionated particles captured from paved surfaces, surface run-off and detention basins. *Science of the Total Environment* **439**, 172–186.

Kuruppu, U., Rahman, A. & Rahman, M. A. 2019 Permeable pavement as a stormwater best management practice: a review and discussion. *Environmental Earth Sciences* **78** (10), 327.

Liu, Y., Li, T. & Peng, H. Y. 2018 A new structure of permeable pavement formitigating urban heat island. *Science of the Total Environment* **634**, 1119–1125.

Maharaj, I. & Elefsiniotis, P. 2001 The role of HRT and low temperature on the acid-phase anaerobic digestion of municipal and industrial wastewaters. *Bioresource Technology* **76** (3), 191–197.

Maniquiz-Redillas, M. C. & Kim, L. H. 2016 Understanding the factors influencing the removal of heavy metals in urban stormwater runoff. *Water Science and Technology* **73** (12), 2921–2928.

Mullaney, J., Rikalainen, P. & Jefferies, C. 2012 Pollution profiling and particle size distribution within permeable paving units – with and without a geotextile. *Management of Environmental Quality* **23** (2), 150–162.

Myers, B., Beecham, S. & van Leeuwen, J. A. 2011 Water quality with storage in permeable pavement basecourse. *Proceedings of the Institution of Civil Engineers-Water Management* **164** (7), 361–372.

Niu, Z. G., Lv, Z. W., Zhang, Y. & Cui, Z. Z. 2016 Stormwater infiltration and surface runoff pollution reduction performance of permeable pavement layers. *Environmental Science and Pollution Research* **23** (3), 2576–2587.

Nnadi, E. O., Newman, A. P. & Coupe, S. J. 2014 Geotextile incorporated permeable pavement system as potential source of irrigation water: effects of re-used water on the soil, plant growth and development. *CLEAN – Soil Air Water* **42** (2), 125–132.

Okochi, N. C. 2013 *Phosphorus Removal From Stormwater Using Electric Arc Furnace Steel Slag*. PhD Thesis, Environmental Systems Engineering, University of Regina, Regina, Saskatchewan, Canada.

Scholz, M. 2013 Water quality improvement performance of geotextiles within permeable pavement systems: a critical review. *Water* **5** (2), 462–479.

Sdiri, A. & Bouaziz, S. 2014 Re-evaluation of several heavy metals removal by natural limestones. *Frontiers of Chemical Science and Engineering* **8** (4), 418–432.

Selbig, W. R., Buer, N. & Danz, M. E. 2019 Stormwater-quality performance of lined permeable pavement systems. *Journal of Environmental Management* **251**, 109510.

Silveira, A. L. L. 2016 Cumulative equations for continuous time Chicago hyetograph method. *RBRH* **21** (3), 646–651.

Welker, A. L., Barbis, J. D. & Jeffers, P. A. 2012 A side-by-side comparison of pervious concrete and porous asphalt. *Journal of the American Water Resources Association* **48** (4), 809–819.

Xie, N., Akin, M. & Shi, X. M. 2019 Permeable concrete pavements: a review of environmental benefits and durability. *Journal of Cleaner Production* **210**, 1605–1621.

Zhang, X. H. 2014 *An Analysis of the Multi-Scale Structure of Rough Surfaces*. MS Thesis, Auburn University, Auburn, AL, USA.

Zhao, Y. & Zhao, C. 2014 Lead and zinc removal with storage period in porous asphalt pavement. *Water SA* **40** (1), 65–72.

Zhao, Y., Zhou, S. Y., Zhao, C. & Valeo, C. 2018 The influence of geotextile type and position in a porous asphalt pavement system on Pb (II) removal from stormwater. *Water* **10** (9), 1205.

First received 31 July 2019; accepted in revised form 27 February 2020. Available online 11 March 2020